Journal of proteome research

pubs.acs.org/jpr

Article

A Multi-omics Longitudinal Study Reveals Alteration of the Leukocyte Activation Pathway in COVID-19 Patients

Kruthi Suvarna, Akanksha Salkar, Viswanthram Palanivel, Renuka Bankar, Nirjhar Banerjee, Medha Gayathri J Pai, Alisha Srivastava, Avinash Singh, Harsh Khatri, Sachee Agrawal, Om Shrivastav, Jayanthi Shastri,* and Sanjeeva Srivastava*

Cite This: https://doi.org/10.1021/acs.jproteome.1c00215

Read Online

ACCESS | Metrics & More | Article Recommendations | Supporting Information

ABSTRACT: Severe coronavirus disease 2019 (COVID-19) infection may lead to lung injury, multi-organ failure, and eventually death. Cytokine storm due to excess cytokine production has been associated with fatality in severe infections. However, the specific molecular signatures associated with the elevated immune response are yet to be elucidated. We performed a mass-spectrometry-based proteomic and metabolomic analysis of COVID-19 plasma samples collected at two time points. Using Orbitrap Fusion LC–MS/MS-based label-free proteomic analysis, we identified around 10 significant proteins, 32 significant peptides, and 5 metabolites that were dysregulated at the severe time points. Few of these proteins identified by quantitative proteomics were validated using the multiple reaction monitoring (MRM) assay. Integrated pathway analysis using distinct proteomic and metabolomic signatures revealed alterations in complement and coagulation cascade, platelet aggregation, myeloid leukocyte activation pathway, and arginine metabolism. Further, we highlight the role of leukocyte activation and arginine metabolism in COVID-19 pathogenesis and targeting these pathways for COVID-19 therapeutics.

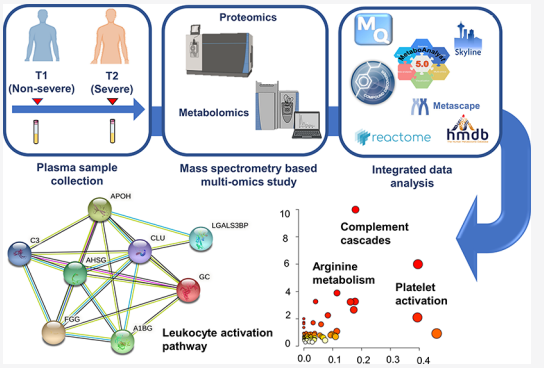

KEYWORDS: *COVID-19, SARS-CoV-2, mass spectrometry, longitudinal, proteomics, metabolomics*

INTRODUCTION

SARS-CoV-2, a highly infectious virus, is responsible for the coronavirus disease 2019 (COVID-19) pandemic, which has substantially impacted the global health and economy. The spectrum of clinical manifestations of COVID-19 ranges from mild or nonsevere to severe life-threatening conditions in a few people. Previous research has revealed the clinical characteristics of COVID-19 and its progression.[1] Patients with mild infection present with common symptoms such as fever, cough, and general weakness, whereas some present with hemoptysis, headaches, and diarrhea. Patients with severe infection exhibit symptoms such as breathlessness with bilateral pneumonia and acute respiratory distress syndrome (ARDS), and in some extreme cases, multiple organ failure due to viremia may eventually lead to death.[2]

The management of COVID-19 includes symptomatic and supportive treatment.[3] The unavailability of drugs targeting COVID-19 led to the reuse of already existing drugs. Moreover, many countries have established evidence-based guideline initiatives that are updated regularly. The most commonly followed strategy is combination therapy, consisting of antiviral (remdesivir, favipiravir), antibiotic (azithromycin), antirheumatic (hydroxychloroquine), antihistamine (cetirizine), anticoagulants (enoxaparin and heparin), anti-inflammatory (dexamethasone), and immunomodulatory (tocilizumab and sarilumab) drugs, which simultaneously inhibits the viral activity and alleviates the symptoms.[4] Moreover, 75% of the hospitalized patients require oxygen supplementation. Thus, oxygen supplementation using noninvasive and invasive ventilation is administered to the patients.[5]

Many patients are likely to undergo nonsevere to severe transitions during their infection period. Previous studies have shown that underlying medical conditions such as diabetes mellitus, hypertension, and other chronic diseases can be the major risk factors for severity progression in some people.[6] Elevated levels of some inflammatory markers such as interleukin-6 (IL-6), D-dimer, C-reactive protein (CRP), and ferritin have been highly correlated with the severity of the disease. Physicians are also considering dynamic changes in

Received: March 17, 2021

other hematological and biochemical markers for determining the condition of COVID-19 patients.[7]

Several omics-based studies have recently increased our understanding of COVID-19 pathophysiology and disease progression and provided a way toward developing better diagnostic and therapeutic approaches.[8,9] Mass spectrometry (MS)-based proteomic and metabolomic approaches have been actively explored to identify biomarkers and therapeutic targets associated with the COVID-19 severity.[10] In our previous study, the comprehensive proteomic analysis of COVID-19 patients revealed significant dysregulation in the pathways related to peptidase activity, regulated exocytosis, blood coagulation, complement activation, and leukocyte activation involved in immune response in severe cases of SARS-CoV-2 infection.[11] Messner et al. used an ultra-high-throughput MS platform for serum and plasma proteomics and identified around 27 potential biomarkers that were differentially expressed in severe cases of COVID-19.[12] Further, Shen et al. performed a comprehensive proteomic and metabolomic analysis of COVID-19 sera and identified dysregulation of multiple immune and metabolic components in severe patients.[13] Although researchers have revealed significant dysregulation of several pathways and biomolecules related to the immune system in severe COVID-19 patients, the key mechanism to be targeted remains unclear.[14] Moreover, most of the studies have been conducted on cohorts of nonsevere and severe patients. A longitudinal study including different time points during the disease progression from the same patients might give us important insights on the potential markers at the individual level.

Longitudinal studies are being conducted globally to provide unique insights about the different stages of their infection, progression toward severe disease, and the mechanism behind these developmental shifts over some time. Demichev et al., in a time-resolved longitudinal proteomic study, identified an age-specific molecular response to COVID-19 involving increased inflammation and lipoprotein dysregulation in older patients.[15] Geyer et al. analyzed serum proteomes of COVID-19 patients in a time-resolved manner. An early decrease in proteins of the innate immune system such as CRP, serum amyloid A1 (SAA1), cluster of differentiation 14 (CD14), lipopolysaccharide-binding protein (LBP), and galectin 3 binding protein (LGALS3BP) was observed during the infection. In contrast, regulators of coagulation [beta-2-glycoprotein 1 (APOH), profilin-1 (PFN1), histidine-rich glycoprotein (HRG), kininogen 1 (KNG1), and plasminogen(PLG)] and lipid homeostasis [apolipoprotein AII (APOA1), APOC1, APOC2, APOC3, and serum paraoxonase/arylesterase 1 (PON1)] increased throughout the disease.[16] Bernardes et al., using a longitudinal multi-omics approach, identified that megakaryocyte and erythroid-cell-derived co-expression modules were predictive of fatal COVID-19 outcome.[17]

Here, we performed a longitudinal analysis of COVID-19 plasma samples collected at two time points: nonsevere and severe. We investigated the changes in the proteome and metabolome at the two time points using MS-based analysis. This is the first longitudinal multi-omics study on the Indian population studying molecular changes during the transition to severe COVID-19. Integrated pathway analysis using distinct metabolomic and proteomic signatures revealed alterations in the complement and coagulation cascade, platelet aggregation, myeloid leukocyte activation pathway, and arginine and proline metabolism at the severe stage of COVID-19 infection. We further highlight the role of leukocyte activation and arginine metabolism in the COVID-19 pathogenesis and targeting these pathways for COVID-19 therapeutics.

MATERIALS AND METHODS

Plasma Sample Collection and Clinical Details

For this study, we procured leftover plasma samples from 13 patients admitted to Kasturba Hospital for Infectious Diseases, Mumbai. The study was approved by the Institute Ethics Committee, IIT Bombay, and Kasturba Hospital for Infectious Diseases Institutional Review Board. The patients were classified as COVID-19 positive based on the COVID-19 RT-PCR test results. As advised by clinicians, based on the progression of the disease, the patients were categorized into the nonsevere to severe transition group. The disease progression was evaluated based on general symptoms, severe respiratory symptoms, SpO2 levels, and need for mechanical ventilation. The nonsevere and severe time points are represented as T1 and T2, respectively. The patient characteristics at different time points are shown in Table S1. The detailed demographic characteristics of the patients are shown in Table S2. After the biochemical tests were performed, the leftover blood (~1 mL) was collected and centrifuged at 3000 rpm for 10 min to separate plasma. The separated plasma was then incubated at 56 °C for 30 min for viral inactivation and further stored at −80 °C in cryovials until further processing. The schematics for sample collection and workflow are shown in Figure 1.

Sample Preparation for Metabolomic Analysis

Plasma samples were collected from nine patients showing nonsevere to severe transition. For severe transitions, we analyzed multiple-time-point plasma samples, which differed from patient to patient. Around 100 μL of plasma separated from the leftover blood sample was dispensed into a sterile tube, and 200 μL of prechilled absolute ethanol was added to the plasma sample. The tube was incubated in a biosafety cabinet for 1.5 h until ethanol was evaporated. To the semi-dried sample, 4× (400 μL) absolute methanol was added and vortexed briefly. The tube was incubated at −20 °C overnight. The next day, the sample was centrifuged at 4 °C for 30 min at 12,000*g*. The supernatant was collected in a fresh tube and stored at −20 °C (Figure 1). Samples were transported at 4 °C to the Proteomics Lab, IIT Bombay. A total of 250 μL of the supernatant was concentrated using a SpeedVac up to a final volume of approximately 80 μL. Fifty microliters of the concentrated sample was dispensed in the glass vial for the MS-based metabolomic profile run. To each glass vial containing 50 μL of the metabolite extract, 0.5 μL of reserpine (10 μg/mL) was added as an internal control for capturing instrumental variation. Vials containing metabolite extract were then placed in an autosampler for metabolite profiling using Q Exactive (Thermo Fisher Scientific, USA).

Metabolomic Analysis Using Ultra-High-Performance Liquid Chromatography

The extracted metabolites with added internal standards were analyzed by an ultra-high-performance liquid chromatography (UHPLC)-MS/MS setup, UHPLC Instrument (Ultimate 3000), coupled with a tandem mass spectrometer (Q Exactive, Thermo Fisher Scientific, USA) with methods using only positive ion electrospray ionization (ESI) mode and a system comprising a HESI (heated ESI) source and an Orbitrap mass

https://doi.org/10.1021/acs.jproteome.1c00215
J. Proteome Res. XXXX, XXX, XXX−XXX

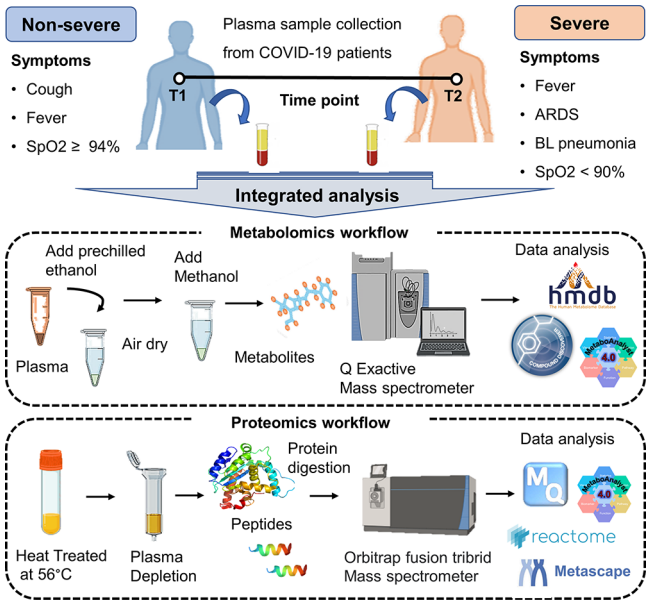

Figure 1. Schematic workflow of the multi-omics-based longitudinal study of COVID-19-infected patient plasma samples. The figure depicts the collection of the longitudinal plasma samples from COVID-19 patients at two time points (T1 and T2), namely, nonsevere and severe, respectively. It also shows the workflow for plasma sample processing for proteomic and metabolomic analysis. For metabolomics, plasma samples were collected from nine patients showing nonsevere to severe transition. We analyzed multiple plasma samples at the severe time point, which differed from patient to patient. The samples were inactivated using ethanol, further processed by the addition of methanol, and analyzed on a Q Exactive mass spectrometer. For plasma proteomic analysis of COVID-19-infected patients, samples from seven patients showing nonsevere to severe transition were taken forward. The plasma was heated at 56 °C for 30 min for viral inactivation, and depletion of highly abundant proteins was performed. The samples were further in-sol digested and processed for label-free quantification using an Orbitrap Fusion mass spectrometer.

analyzer. The resolution for the mass spectrometer was set to be 140,000 and 17,500 for full MS and ddMS2, respectively, and was scanned within 100 to 700 m/z mass range. A Hypersil Gold column (C18, 100 × 2.1 mm, 1.9 μm particle size, Thermo Fisher Scientific, USA) was used along with water and absolute methanol with 0.1% formic acid (FA) as the eluent solvent. The capillary temperature was set at 34 °C with aux gas rate at 10 and sheath gas flow at 42. A 20 min gradient was used with different concentrations of methanol flowing at 0.350 mL/min, reaching at different times are as follows: 1% at 2 min, 50% at 5 min, 98% at 14 min, and maintained till 17th min, 1% at 17.2 min and maintained till 20th min. Samples were run in batches, with every batch having an initial blank of resolving solvent (50% methanol), and the same blank was run after all samples of a particular patient. Every sample was run in technical triplicates in both MS only and MS2 modes. Quality check control samples were also run after every five sets of sample technical replicates, which were made from the pool of the samples run in the batch.

Metabolomic Data and Statistical Analysis

The raw data acquired from the mass spectrometer were primarily analyzed in the Compound Discoverer (CD) 3.0 software (Thermo Fisher) for metabolite identification/quantitation, chromatography peak alignment, mass spectrum visualization, and further statistical analysis. The standard workflow template was used in CD having unknown compound detection with a signal-to-noise (S/N) ratio of 3, peak alignment keeping a minimum peak intensity threshold at 10^6, predicting the composition of the compound, and database searching against ChemSpider, comprising of BioCyc, KEGG, and Human Metabolome Database (HMDB) with a mass tolerance of 5 ppm. Apart from ChemSpider, mzCloud and Metabolika were also used as the data sources for compound annotation. Further, statistical analysis was performed mostly using the MetaboAnalyst web-based software. Different batches of QC pools and internal standards were used to determine the further normalization strategies. Spearman rank correlation analyses were used to check data quality, and samples that have an R^2 of at least 0.5 were further considered. Features having less than 30% missing values in each cohort were considered further with imputing missing values with KNN (k-nearest neighbors). After merging the imputed data of both cohorts, the data were median-normalized and log-transformed followed by a two-tailed unpaired t test with false discovery rate (FDR) adjusted values, a p value threshold less than 0.05, and log2 fold-changes with a minimum threshold of 1.5 to determine statistically significant differentially expressed metabolites. These significant metabolites were further checked for their correlations with heat maps and principal component analysis (PCA) plots.

Sample Preparation for Proteomic Analysis

For plasma proteomic analysis of COVID-19-infected patients, samples from seven patients showing nonsevere to severe transition were taken forward. Around 15 μL of plasma samples were first subjected to a Pierce Top 12 Abundant Protein Depletion Spin Column (Thermo Fisher Scientific) to deplete highly abundant proteins and incubate for 1 h using a rotating shaker. The depleted plasma samples were eluted by centrifugation at 1500g for 2 min. The samples were further concentrated to one-fourth of their initial volume using a SpeedVac (Thermo Fisher Scientific). The protein concentration in the depleted plasma samples was quantified using the Bradford assay. Then, approximately 30 μg of the depleted plasma sample was taken forward for in-solution digestion. The samples were dried using a SpeedVac and dissolved in 10 μL of 6 M urea buffer. The plasma proteins were reduced with TCEP (final concentration 20 mM) at 37 °C for 1 h and then alkylated with iodoacetamide (final concentration 40 mM) for 15 min under dark conditions. The samples were diluted six times with 50 mM ammonium bicarbonate before digestion. Proteins were subjected to enzymatic digestion using trypsin at an enzyme/substrate ratio of 1:30 for 16 h at 37 °C. The digested peptide was then vacuum dried and reconstituted in 0.1% (v/v) FA. Further, the digested peptides were desalted using the C18 column. The desalted peptides were further dried and dissolved in 0.1% (v/v) FA. The peptide concentration was calculated using the Scopes method using absorbance at 205 and 280 nm.

Proteomic Analysis Using Label-Free Quantification

One microgram of the peptide sample was run in the Orbitrap Fusion Tribrid Mass Spectrometer (Thermo Fisher Scientific) with the EASY-nLC 1200 system with a gradient of 80% acetonitrile (ACN) and 0.1% FA for 120 min with blanks after every sample. Bovine serum albumin (BSA) was run at the start and end point of each set of the run to check the

https://doi.org/10.1021/acs.jproteome.1c00215
J. Proteome Res. XXXX, XXX, XXX−XXX

instrument quality. All samples were loaded onto the LC column at a flow rate of 300 nL/min. Mass spectrometric data acquisition was done using the data-dependent acquisition mode with a mass scan range of 375−1700 m/z and mass resolution of 60,000. A mass window of 10 ppm was set with a dynamic exclusion of 40 s. All MS/MS data were acquired by the high energy collision dissociation method of fragmentation, and data acquisition was performed using the Thermo Xcalibur software version 4.0.

Proteomic Data Analysis and Statistical Analysis

All the raw data sets obtained from the instrument were processed with MaxQuant (v1.6.6.0)[18] and searched with the built-in Andromeda search engine against the Human Swiss-Prot database (downloaded on 09/07/2020), which contains a total of 20,353 proteins. The label-free-quantification parameters were used to process the raw files and label-type setting as ″standard″ with a multiplicity of one. Fusion mode was set in the Orbitrap, and trypsin was used for digestion with a maximum missed cleavage of two. The carbamidomethylation of cysteine (+57.021464 Da) was set as the static modification, and the oxidation of methionine (+15.994915 Da) was set as the variable modification. FDR was set as 1% for the identification of protein and peptide with high reliability. The decoy mode was set to ″reverse″, and the type of identified peptides was set as ″unique + razor″ (Table S3). The MaxQuant output file included data for seven patients at two time points used for the statistical analysis. A sample-wise correlation was performed to understand the data quality. Subsequently, data were taken forward for the 50% missing value imputation using the k-nearest neighbor (KNN) method in MetaboAnalyst.[19] Further, analysis was performed using Microsoft Excel, log2 fold-change in the intensities was taken forward, and Welch's t test was calculated. The proteins having a p value less than 0.05 and log2 fold-change greater than ±1.2 were considered significant proteins. Further, the peptide analysis was done using MetaboAnalyst without any missing value imputation, and the peptides having a p value less than 0.05 were taken forward.

Targeted Proteomics by Multiple Reaction Monitoring (MRM) Assay

The proteins found to be of statistical significance during the LFQ were selected and used for a targeted MRM study. The list of transitions was prepared for unique peptides of these selected proteins using Skyline-daily (version 20.2.1.404). The missed cleavage criterion was 0. In the transition settings precursor charges were +2, +3, and product charges were set at +1 and +2. Only ion transitions were included in the list. Pooled samples of both time points were run against the generated transitions. Based on these runs, a list was finalized. This list included a spiked-in synthetic peptide (THCLYTHVCDAIK) essential for monitoring the consistency of the MS runs. A Vanquish UHPLC system (Thermo Fisher Scientific, USA) connected to a TSQ Altis Mass Spectrometer (Thermo Fisher Scientific, USA) was used for the experiment. The peptides were separated using a Hypersil Gold C18 column (1.9 μm, 100 × 2.1 mm, Thermo Fisher Scientific, USA) at a flow rate of 0.45 mL/min for a total time of 10 min. The binary buffer system consisted of 0.1% FA as buffer A and 80% ACN in 0.1% FA as buffer B. Approximately 300 ng of BSA was also run with the samples to check for uniformity in the instrument response.

Integrated Pathway Analysis

The integrated pathway analysis was performed using MetaboAnalyst. The Gene Ontology (GO) enrichment analysis was performed in Metascape,[20] and the proteins mapped on the biological pathway were taken forward for visualization. STRING (version 11)[21] and Reactome (version 73)[22] were used to perform the protein−protein interaction analysis and pathway mapping, respectively.

Data Availability

All proteomic data associated with this study are present in the manuscript or the supplementary materials. Raw MS data and search output files for proteomic data sets are deposited on the Proteome Xchange Consortium via the PRIDE[23] partner repository (PRIDE ID: PXD023521). The metabolomic data are deposited on metaboLights (ID: MTBLS2469). Targeted proteomic data is deposited on Panorama Public, and it can be accessed using the access URL https://panoramaweb.org/longitudinal_plasma_MRM.url.

RESULTS

Trends of the Clinical Parameters during COVID-19 Progression

Laboratory tests for clinical markers aid the clinicians in the diagnosis and management of the disease. In our study, serum CRP, aspartate aminotransferase (AST), cell count, bilirubin, and IL-6 levels were monitored for patients with severe disease to better manage COVID-19 (Figure S1 and Table S2). The blood cell counts revealed that the total cell count was elevated during the severe stage as compared with the nonsevere stage of the disease. Moreover, the polymorphonuclear leukocytes were found to be increased, whereas lymphopenia was observed to be decreased, throughout the course of the disease. The serum AST levels were higher than the normal values throughout the course of the disease. The CRP, IL-6, D-dimer, and ferritin were monitored for patients showing severe symptoms; we observed that serum levels were elevated for all these parameters. The patients included in the study were prescribed a combination of antibacterial or antiviral agents to treat most patients with mild symptoms. Anticoagulants (Clexane) and low doses of the immunomodulatory drug methylprednisolone (MPS) were given to some patients with mild symptoms. Remdesivir, an RNA polymerase inhibitor, was administered mostly to patients with severe symptoms. Almost all the patients with severe symptoms were administered immunomodulatory drugs such as MPS and tocilizumab. These results suggest that the trends for some of the clinical markers remained above the normal range for samples collected at the severe time point despite the treatment with the immunomodulatory drugs.

A Significant Alteration of Metabolites during Nonsevere to Severe Transition Points of COVID-19 Infection

Of the total of nine patient samples used for the metabolomic study, one sample showed poor quality; hence, eight patient samples were taken for analysis. On analysis of 15 multiple severe time points and 9 nonsevere time points from 8 COVID-19 patients, 5 metabolites were found to be differentially expressed metabolites (DEMs) and had FDR-adjusted p values less than 0.05 and fold change cutoff >1.5 showing both upregulated and downregulated metabolites (Table S4). QC checks for the sample run using the internal standard (reserpine) are shown in Figure S2. The samples from

https://doi.org/10.1021/acs.jproteome.1c00215
J. Proteome Res. XXXX, XXX, XXX−XXX

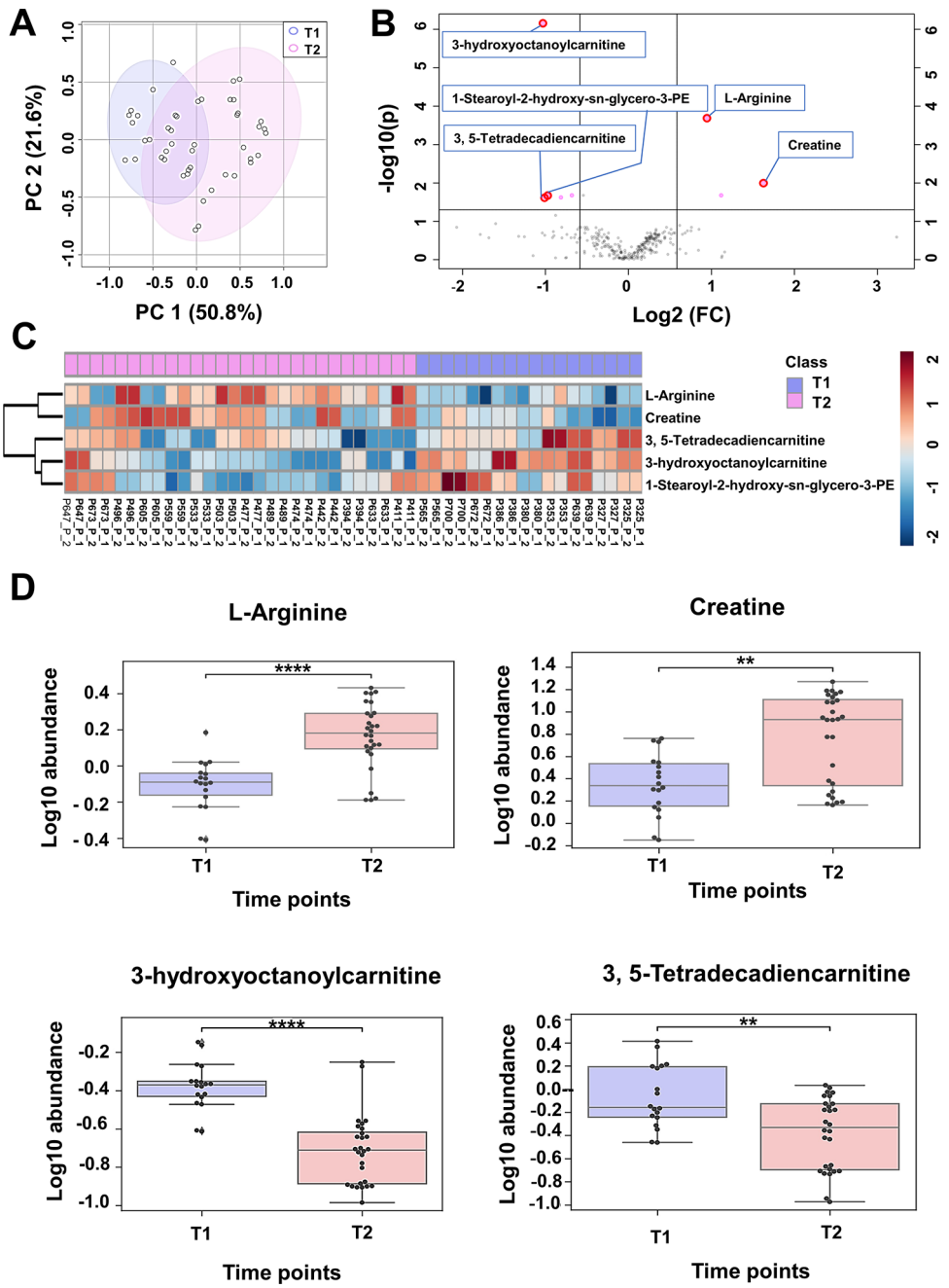

Figure 2. Significant alteration of metabolites during nonsevere to severe transition points of COVID-19 infection. For metabolomics, plasma samples were collected from nine patients showing nonsevere (T1) to severe (T2) transition. We analyzed multiple plasma samples at the severe time point (T2); the sampling differed from patient to patient. (A) The PCA plot showing the segregation into two clusters: nonsevere and severe. (B) The volcano plot showing the significant differentially expressed metabolites (DEMs) in severe vs nonsevere. (C) The heat map of five significant DEMs in severe vs nonsevere time point. All the samples were run in technical duplicates. (D) The box plots for four of these metabolites (L-arginine, creatine, 3-hydroxyoctanoylcarnitine, and 3,5-tetradecadiencarnitine) are shown for two time points. Welch's *t* test ns: $5.0 \times 10^{-2} < p \leq 1.0 \times 10^{0}$, *: $1.0 \times 10^{-2} < p \leq 5.0 \times 10^{-2}$, **: $1.0 \times 10^{-3} < p \leq 1.0 \times 10^{-2}$, ***: $1.0 \times 10^{-4} < p \leq 1.0 \times 10^{-3}$, ****: $p \leq 1.0 \times 10^{-4}$.

severe and nonsevere time points were segregated as two clusters using PCA (Figure 2A). The volcano plot showing the significant DEMs is shown in Figure 2B. Of the eight metabolites, all except one were adjudged noncontaminant from the blank solvent. Additionally, five of these metabolites (L-arginine, creatine, 3-hydroxyoctanoyl carnitine, 3,5-tetradecadien carnitine, and 1-stearoyl-2-hydroxy-*sn*-glycero-3-PE) were level-2 MSI, their spectra matching with online databases of MassBank of North America (MoNA) and the Human Metabolome Database (HMDB). The heat map showed that five metabolites segregated the severe and nonsevere COVID-19 sample sets (Figure 2C). These metabolites were identified to significantly alter at the severe time point (Figure 2D and Figure S3). In line with our findings, few researchers have also observed an increase in the level of L-arginine and creatine in the COVID-19 patients (Table S5). Thus, the dysregulation of these biomolecules suggests that SARS-CoV-2 might play an important role in the alteration of the metabolism in the infected host.

https://doi.org/10.1021/acs.jproteome.1c00215
J. Proteome Res. XXXX, XXX, XXX−XXX

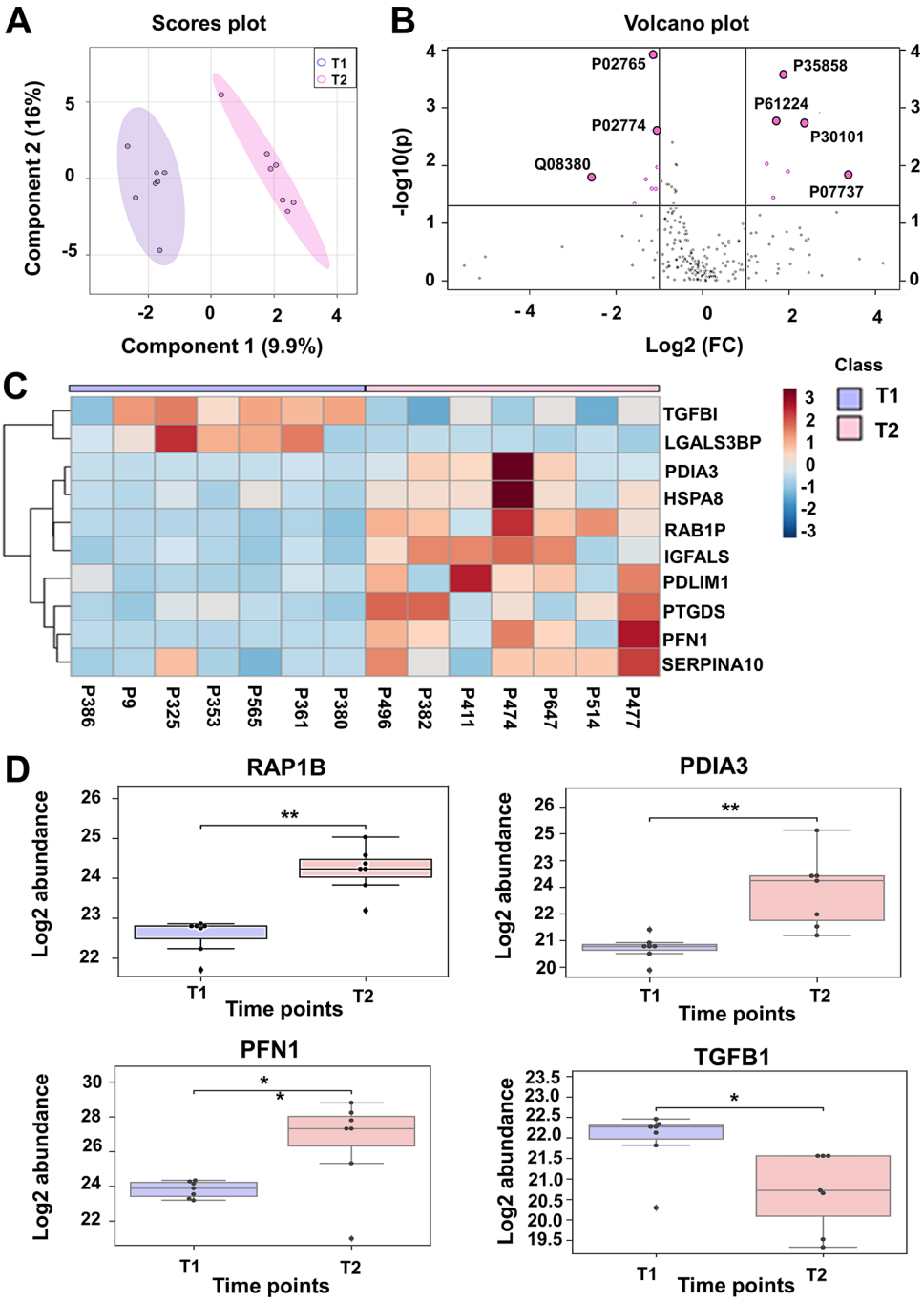

Figure 3. Significant alteration of proteins during nonsevere to severe transition points of COVID-19 infection. For plasma proteomic analysis of COVID-19-infected patients, samples from seven patients showing nonsevere (T1) to severe (T2) transition were taken forward. (A) The partial least squares-discriminant analysis (PLS-DA) plot showing the segregation into two clusters: nonsevere and severe (T1 and T2), respectively. (B) The volcano plot showing the significant differentially expressed proteins (DEPs) in severe vs nonsevere. (C) The heat map of 10 significant DEPs at severe vs nonsevere time point. (D) The box plots for four of these proteins (RAP1B, PDIA3, PFN1, and TGFB1) are shown for two time points. Welch's *t* test *: $1.0 \times 10^{-2} < p \leq 5.0 \times 10^{-2}$ and **: $1.0 \times 10^{-3} < p \leq 1.0 \times 10^{-2}$.[4] $< p \leq 1.0 \times 10^{-3}$, ****: $p \leq 1.0 \times 10^{-4}$

A Significant Alteration of Proteins during Nonsevere to Severe Transition Points of COVID-19 Infection

The total proteins and peptides identified in each COVID-19 patient sample on LFQ analysis are shown in Figure S4. The total number of proteins common and unique to samples from T1 and T2 time points is shown in the form of a Venn diagram (Figure S5). The T1 and T2 time points segregated into two distinct clusters on partial least squares-discriminant analysis (PLS-DA) for 14 samples (Figure 3A). Statistical analysis between the two time points identified a list of 10 differentially expressed proteins passing the significant criteria that are represented in the volcano plot (Figure 3B) and heat map (Figure 3C). In particular, Ras-related protein Rap-1b (RAP1B), insulin-like growth factor-binding protein complex (IGFALS), protein disulfide-isomerase A3 (PDIA3), heat shock cognate 71 kDa protein (HSPA8), PDZ and LIM domain protein 1 (PDLIM1), profilin-1 (PFN1), prostaglandin-H2 D-isomerase (PTGDS), and protein Z-dependent

https://doi.org/10.1021/acs.jproteome.1c00215
J. Proteome Res. XXXX, XXX, XXX−XXX

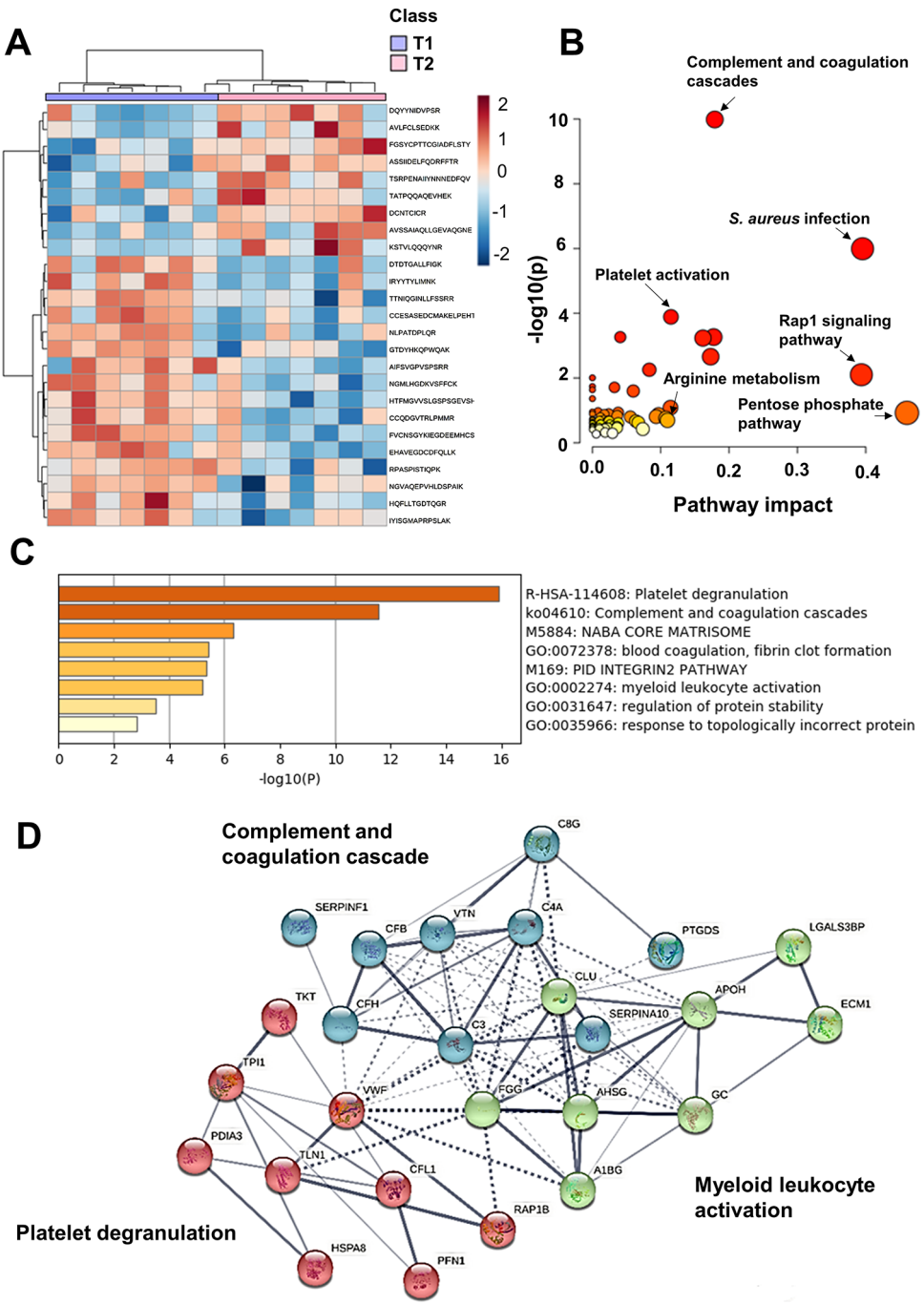

Figure 4. Mapping of significant proteins, peptides, and metabolites for identification of altered pathways at severe time points. (A) Heat map of significant peptides mapping to the proteins using peptide analysis. (B) The integrated pathway analysis using MetaboAnalyst showed dysregulation of the following pathways: complement and coagulation cascades, platelet activation, Rap1 signaling pathway, and arginine metabolism. (C) The Metascape pathway analysis shows dysregulation of pathways such as platelet degranulation, complement and coagulation cascades, blood coagulation, fibrin clot formation, integrin pathways, myeloid leukocyte activation, regulation of protein stability, and response to topologically incorrect proteins. (D) The proteins mapping to the prominent pathways are shown in the STRING network.

protease inhibitor (SERPINA10) were upregulated, and transforming growth factor-beta-induced protein (TGFBI) and LGALS3BP were downregulated (Table S6). These proteins were found to be significantly altered at the severe time points (Figure 3D and Figure S6), indicating that these proteins might play an important role in maintaining SARS-CoV-2 proliferation in the host.

Integrated Pathway Analysis Revealed a Significant Dysregulation of Leukocyte Activation and Arginine Metabolism

We observed around 32 significant peptides mapping to the proteins PDZ and LIM domain protein 1 (PDLIM1), complement C3 (C3), fibrinogen gamma chain (FGG), beta-2-glycoprotein 1 (APOH), alpha-2-HS-glycoprotein (AHSG), vitamin D-binding protein (GC), alpha-1B-glycoprotein (A1BG), von Willebrand factor (VWF), profilin-1 (PFN1),

https://doi.org/10.1021/acs.jproteome.1c00215
J. Proteome Res. XXXX, XXX, XXX−XXX

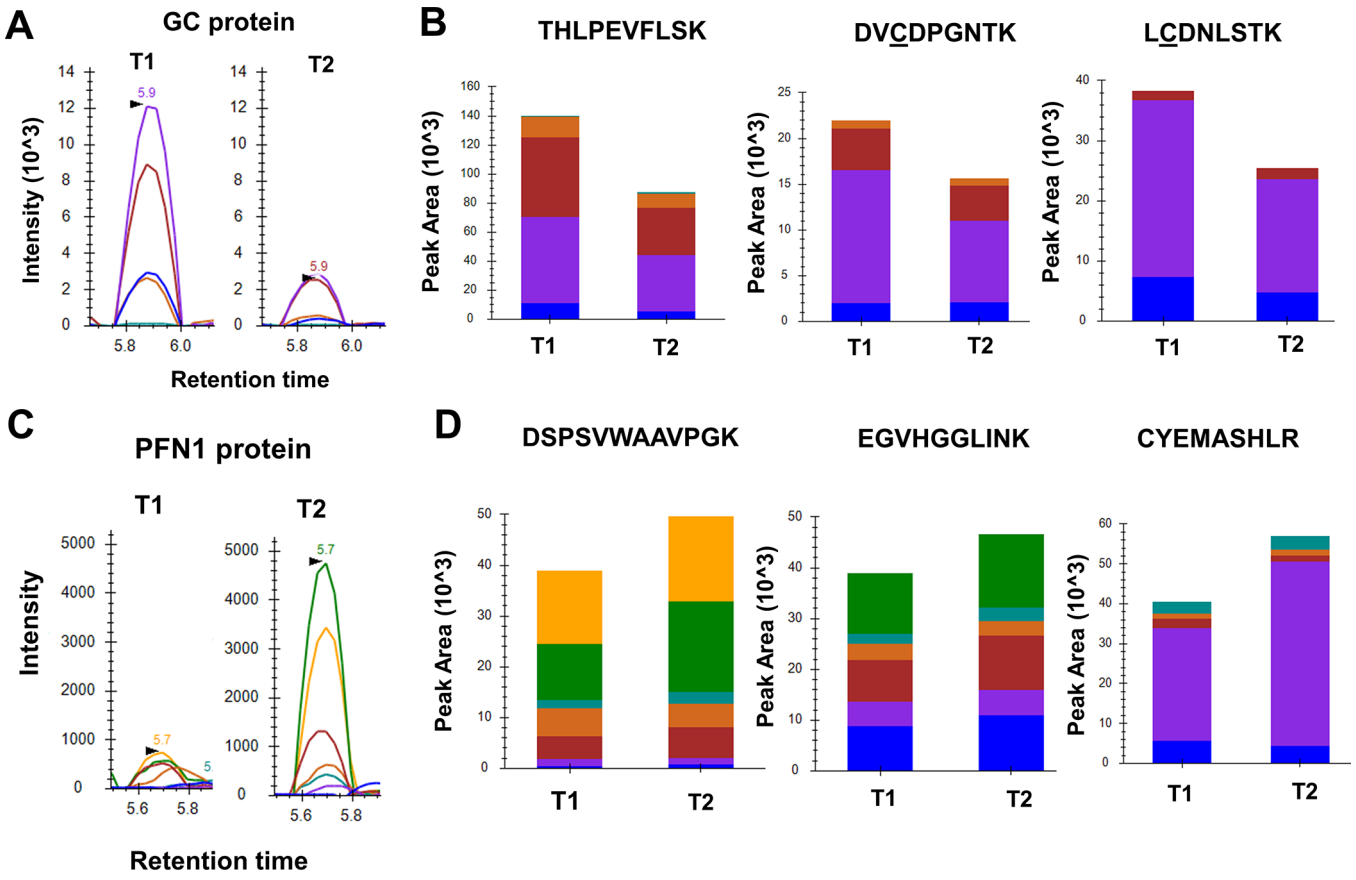

Figure 5. Validation of proteins detected by LFQ using the MRM assay. (A) Representative MRM peaks for a peptide of the GC protein showing the downregulation in the severe time point (T2) sample compared to the nonsevere time point (T1) sample from a COVID-19 patient. (B) Bar plots for three peptides (THLPEVFLSK, DVCDPGNTK, and LCDNLSTK, respectively) of the GC protein showing the downregulation. (C) Representative MRM peaks for a peptide of the PFN1 protein showing the upregulation in the T2 sample as compared the T1 sample from a COVID-19 patient. (D) Bar plots for three peptides (DSPSVWAAVPGK, EGVHGGLINK, and CYEMASHLR, respectively) of the PFN1 protein showing the upregulation.

complement factor H (CFH), complement C1s subcomponent (C1S), complement C4-A (C4A), histone H1.4 (H1-4), clusterin (CLU), histone H1.2 (H1-2), filamin-A (FLNA), transketolase (TKT), pigment epithelium-derived factor (SERPINF1), triosephosphate isomerase (TPI1), galectin-3-binding protein (LGALS3BP), EGF-containing fibulin-like extracellular matrix protein 1 (EFEMP1), leukocyte immunoglobulin-like receptor subfamily A member 3 (LILRA3), proteoglycan 4 (PRG4), and talin-1 (TLN1). The heat map of these proteins is shown in Figure 4A. The list of these significant peptides is shown in Table S7. The integrated pathway analysis using MetaboAnalyst showed dysregulation of the following pathways: complement and coagulation cascades, platelet activation, focal adhesion, Rap1 signaling pathway, antigen processing and presentation, mitogen-activated protein kinase signaling pathway, and arginine and proline metabolism (Figure 4B and Table S8). The pathway analysis using Metascape showed dysregulation of platelet degranulation, complement and coagulation cascades, blood coagulation, fibrin clot formation, integrin pathways, myeloid leukocyte activation, regulation of protein stability, and response to topologically incorrect protein pathways (Figure 4C and Table S9). Proteins mapping to the complement and coagulation cascade (C1S, C3, C4B, CLU, FGG, CFH, VWF, APOH, AHSG, IGFALS, SERPINA10, SERPINF1, RAP1B, and LILRA3), platelet degranulation (A1BG, AHSG, APOH, CLU, FGG, VWF, FLNA, and PFN1), and myeloid leukocyte activation (A1BG, AHSG, C3, CLU, HSPA8, RAP1B, LILRA3, and PDIA3) are represented in a network using STRING (version 11) (Figure 4D). The representative figure for the prominent pathways from Reactome.org is shown in Figures S7−S9. Here, we focus on an important role of amino acid metabolism and leukocyte activation pathway during SARS-CoV-2 infection.

Validation of LFQ Identified Significant Proteins Using the MRM Approach

Further, MRM assay was used to validate the differentially regulated proteins identified in the LFQ analysis using seven longitudinal severe and nonsevere depleted plasma samples. An equal amount of a heavy labeled synthetic peptide (THCLYTHVCDAIK) was spiked in all samples to ensure a consistent response from the injections. The uniform peak areas observed for this peptide are shown in Figure S10. Using the MS Stats external tool in Skyline, we determined that the vitamin-D-binding protein (GC) protein (THLPEVFLSK, DVCDPGNTK, and LCDNLSTK) was down-regulated in the severe COVID-19 patient samples (Figure 5A,B), and PFN1 (DSPSVWAAVPGK, EGVHGGLINK, and CYEMASHLR) was identified to be upregulated (Figure 5C,D). However, further validation and absolute quantification of the identified peptides on a larger cohort of samples are required to reach a firm conclusion.

https://doi.org/10.1021/acs.jproteome.1c00215
J. Proteome Res. XXXX, XXX, XXX−XXX

DISCUSSION

We conducted a longitudinal multi-omics study of a small cohort (n = 13) using plasma samples collected at two time points, namely, nonsevere and severe. With limited knowledge and the dynamic nature of COVID-19 infection, monitoring clinical parameters becomes inevitable while treating the patients. Recently, Velavan et al. have summarized that the laboratory parameters such as low lymphocyte count and serum CRP, D-dimer, ferritin, and IL-6 levels can help in predicting severe and fatal COVID-19 outcomes.[24] In our previous proteomic study, we have observed an increase in the expression of IL-6 and CRP in severe patients using swab samples.[25]

In a meta-analysis by Moutchia et al., they reported that severe COVID-19 infection is associated with an increased neutrophil count and IL-6 and CRP levels, and decreased lymphocyte count. Previously, moreover, they also suggested that increased D-dimer, AST, alanine aminotransferase (ALT), urea, and creatinine could be used for stratifying severe patients with COVID-19 infection.[26] Similar to their findings, our clinical data showed a high level of serum CRP, AST, bilirubin, and interleukin 6 (IL-6) in the patients with severe COVID-19 infection (Figure S1). The serum levels for these clinical parameters were above the normal range during the severe time point even after the administration of immunomodulatory drugs. Lymphopenia was also reported in patients during the severe and nonsevere stages of the disease. Although these parameters have been able to guide clinicians in predicting the course of the disease, the pathogenesis of the disease remains unclear. At such times, there is an urgent need to use multi-omics approaches for identifying the altered biomolecular profile and associated biological pathways that lead to severe symptoms in the SARS-CoV-2-infected host.

In this study, we performed a high-throughput mass-spectrometry-based proteomic and metabolomic analysis for the identification of altered biomolecules and pathways in the severe COVID-19 longitudinal samples (Figure 1). So far, only a few studies have used a multi-omics approach for a longitudinal study of the COVID-19 infection.[9,17] The metabolomic analysis was performed on eight COVID-19 patient samples collected at multiple time points during progression from nonsevere to a severe state. The metabolomic investigation of infected plasma samples revealed a significant alteration of L-arginine, creatine, 3-hydroxyoctanoyl carnitine, 3,5-tetradecadien carnitine, and 1-stearoyl-2-hydroxy-*sn*-glycero-3-PE (Figure 2). Fraser et al., in their COVID-19 metabolomic study, revealed that either creatinine alone or a creatinine/arginine ratio could predict ICU mortality with 100% accuracy.[27] Similar to their finding, we observed a significant upregulation of both creatine and arginine at severe time points. However, the creatinine breakdown product of creatine was not found to be significant in our analysis. The elevated serum creatinine levels have been an indicator of kidney dysfunction in the severe cases of COVID-19 infection leading to fatal outcomes.[28,29] Along with the increase in creatine, the clinical parameters also suggest the increase in the bilirubin and AST level at severe time points. Recently, Rosa et al. showed that the SARS-CoV-2 spike protein binds to bilirubin: thus, it might have a role in SARS-CoV-2 immune invasion.[30] Although bilirubin itself was not identified in our metabolomic analysis, this might indicate that SARS-CoV-2 significantly alters the metabolism in the host. Tang et al. identified that patients showing an increase in levels of 3-hydroxyoctanoyl carnitine and 3,5-tetradecadien carnitine metabolites were at high risk of developing heart failure.[31] Since most of the patients with severe COVID-19 infection eventually die of multiorgan failure, these metabolites might be a potential indicator of disease progression and fatal outcomes.

Recently, few researchers performed a longitudinal proteomic profile and revealed a significant alteration in proteins involved in the regulation of the immune system (Table S10).[15,16] In this study, the proteomic analysis of longitudinal samples revealed 10 significant proteins and 35 significant peptides to be altered at the severe time point. The significant proteins identified were RAP1B, IGFALS, PDIA3, HSPA8, PDLIM1, TGFBI, LGALS3BP, PFN1, PTGDS, and SERPINA10 (Figure 3). We observed a few proteins such RAP1B, PDIA3, and PFN1 that play an important role in platelet function and thrombosis to be significantly upregulated in severe patients.[32−34] The small molecule mediated inhibition of PDIA3 during influenza infection has been reported to decrease the viral load and improve lung inflammation.[35] Thus, these proteins can be explored as potential targets for COVID-19 therapeutics. Proteins such as TGFB1 and LGALS3BP were identified to be significantly suppressed in severe patients. Interestingly, the recent transcriptomics-based longitudinal study also identified persistent downregulation of TFGB1 transcripts in severely ill COVID-19 patients.[17] Gutmann et al. demonstrated that LGALS3BP is a novel putative binding partner of the SARS-CoV-2 spike glycoprotein and possesses antiviral activity.[36] Thus, the decrease in the level of these proteins might indicate the progression toward severity. However, it cannot be ruled out that the decrease might also be the outcome of treatments administered to severe patients.

Further, the integrated pathway analysis from significant proteins and metabolome identified in the severe patients showed predominant dysregulation of complement and coagulation cascades, platelet activation and degranulation, myeloid leukocyte activation, and arginine amino acid metabolism (Figure 4). We observed that components of the classical complement pathway (C1S and C4B), C3, and complement modulator (CFH) were modulated at the severe time point. Moreover, other proteins such as RAP1B, IGFALS, and SERPINA10, an inhibitor of the F10a coagulation factor, were also significantly dysregulated. The complement cascade is one of the sentinels of the innate immune system. It plays a major role in the defense against invading pathogens by recruiting immune cells to sites of infection, labeling the invading pathogens via opsonization for uptake and destruction by phagocytes, and direct lysis of susceptible pathogens.[37] Dysregulation of this cascade can contribute to inflammation-mediated pathologies. Similarly, inflammation-induced coagulation pathways are pivotal in controlling the pathogenesis associated with COVID-19 infections.[38]

Dysregulations of complement component C3 have been reported to cause severe forms of COVID-19. Moreover, the inactivation of C3 has been reported to ameliorate lung injury due to the upstream positioning of C3 signaling in the innate immune cascade. Therefore, C3 can be considered as a biomarker for systemic inflammation, and its inhibition can potentially control COVID-19 associated with acute respiratory distress.[39] Moreover, Messner et al. reported that C1S and CFH were activated in COVID-19 patients. They also reported the upregulation of SERPINA10.[12] Furthermore, D'Alessandro et al. also reported the upregulation of CFH in COVID-19

https://doi.org/10.1021/acs.jproteome.1c00215
J. Proteome Res. XXXX, XXX, XXX−XXX

patients.[40] These observations indicate that the complement cascade plays a major role in the pathogenesis of COVID-19 and can be a potential target for drug therapy.

We also observed the alteration in proteins such as FGG, VWF, FLNA, PFN1, and LGALS3BP involved in platelet activation and degranulation. Fibrinogen is an oligomeric glycoprotein produced in the liver and secreted into the blood. Fraga et al. observed that increased fibrin formation and lysis account for high levels of D-dimers and are associated with worse outcomes in patients with COVID-19.[41] Furthermore, Ruberto et al. observed a marked increase in the binding of active VWF to platelets in severe patients.[42] Thus, these proteins might predict the fatal complications and can also be explored for the therapeutic potential.

Interestingly, we also identified the dysregulation of proteins such as A1BG, AHSG, C3, CLU, HSPA8, RAP1B, LILRA3, and PDIA3 involved in the myeloid leukocyte activation pathways. Myeloid cells represent a diverse range of innate leukocytes crucial for mounting successful immune responses against viruses. These cells are responsible for detecting pathogen-associated molecular patterns, thereby initiating a signaling cascade that results in the production of cytokines such as interferons to mitigate infections.[43] Schulte-Schrepping et al. performed single-cell RNA-sequencing and proteomics of whole-blood and peripheral-blood mononuclear cells to determine changes in immune cell composition and activation in mild versus severe COVID-19. They observed a high occurrence of neutrophil precursors as evidence of emergency myelopoiesis and dysfunctional mature neutrophils in the severe COVID-19 patients.[44] These studies support the observation of myeloid leukocyte activation in severe patients.

When an antiviral immune response is generated, a balance must be reached between two opposing pathways: the production of proinflammatory and cytotoxic effectors that drive the robust antiviral immune response to control the infection and regulators that function to limit or blunt an excessive immune response to minimize immune-mediated pathology and repair tissue damage.[45] Myeloid cells, including monocytes and macrophages, play an important role in this balance, particularly through the activities of the arginine-hydrolyzing enzymes nitric oxide synthase 2 (Nos2; iNOS) and arginase 1 (Arg1).[46] We identified the dysregulation of both arginine metabolism and myeloid leukocyte activation at the severe time point, indicating that the imbalance between these pathways might be responsible for the fatal symptoms of cytokine storm seen in the COVID-19 patients. Thus, this study reveals that leukocyte activation and amino acid metabolism can be beneficial and damaging to the COVID-19 infection.

Recently, there has been an unprecedented increase in understanding the role of small molecule metabolites in SARS-CoV-2 replication and proliferation in the host (Table S5). The comprehensive metabolomic studies of infected patient sera samples have revealed substantial alterations in fatty acid and amino acid metabolism, specifically pathways involved in the metabolism of tryptophan, arginine, and lysine.[47−49] Most of these studies were performed in the small cohort of COVID-19 positive and negative patients. Barberis et al. performed one of the largest untargeted metabolomic analysis using plasma samples; they observed a significant alteration in phenylalanine and tyrosine metabolism in noncritical COVID-19 patients.[50] Although these studies have significantly increased the understanding of infection, a longitudinal study is important for developing personalized medicine. Importantly, in our longitudinal analysis focusing on nonsevere to severe transition, we identified amino acid metabolism, essentially arginine metabolism, to be the significant pathway altered in the host. Similar to our finding, Ansone et al. in their longitudinal targeted metabolomic study of serum samples identified the role of arginine metabolism in the immune response to SARS-CoV-2 and linked it to the acute phase response and disturbed kidney function observed in the severe patients.[51] However, unlike in our study, the alteration in the level of L-arginine itself was not detected; rather, an alteration of citrulline and ornithine amino acid involved in the arginine catabolism was identified. In another study, Xiao et al. revealed a significant correlation between circulating inflammatory cytokines such as IL-6, IP-10, and M-CSF and the metabolites involved in arginine metabolism in severe patients.[52] Thus, these studies support our findings and indicate that the development of therapeutics for targeting the amino acid metabolism pathway might aid in suppressing the elevated immune response.

Additionally, we validated significant peptides mapping to PFN1 and the vitamin D-binding protein (GC) protein identified in the proteomic study using the MRM approach. Interestingly, we observed that three peptides mapping to the GC protein were significantly downregulated in the severe patients (Figure 5). Vitamin D deficiency has been reported as a key factor in developing respiratory tract infections and inflammatory processes like acute respiratory distress syndrome.[53] Speeckaert et al. reported that vitamin D binding protein, the major carrier of vitamin D, probably plays an underestimated role in the pathogenesis of COVID-19. Lower serum vitamin D-binding protein levels were associated with a higher risk of in-hospital mortality.[54] Therefore, this suggests the importance of vitamin D supplementation during the treatment of COVID-19.

In summary, this longitudinal study identified the distinct proteomic and metabolomic profile for the prognosis of COVID-19 severity. This study also revealed that arginine metabolism and immune response mechanism, specifically the leukocyte activation pathway, are strongly linked to the fatal symptoms induced by the SARS-CoV-2 infection. Thus, along with strengthening the data resources generated, the biomolecular pathways identified might be explored for novel therapeutic interventions.

CONCLUSIONS

The leukocyte activation pathway and arginine metabolism might play a key role in predicting fatal outcomes and could be considered for COVID-19 therapeutic interventions. However, the study has its limitation in the sample size. The small cohort necessitates further validation using a larger cohort before extrapolating the results for clinical application. Moreover, the patients in this study received immune-modulatory drug therapy; thus, the proteomic or metabolomic response might be due to the therapeutic outcome. Nonetheless, this is the first longitudinal study in an Indian population; it can benefit the researchers trying to decipher the immune response and characteristics of a population to COVID-19 infections.

https://doi.org/10.1021/acs.jproteome.1c00215
J. Proteome Res. XXXX, XXX, XXX−XXX

■ ASSOCIATED CONTENT

Supporting Information

The Supporting Information is available free of charge at https://pubs.acs.org/doi/10.1021/acs.jproteome.1c00215.

Clinical characteristics of the patients used in the study (Table S1); demographic characteristics of COVID-19-infected patients at two time points (T1 and T2) (Table S2); MaxQuant analysis parameter file (Table S3); list of significant metabolites at severe time points (Table S4); an overview of metabolomic techniques revealing the mechanism of SARS-CoV-2 infection in the host (Table S5); list of significant proteins at severe time points (Table S6); list of significant peptides at severe time points (Table S7); integrated pathway analysis using MetaboAnalyst (Table S8); list of significant pathways identified using Metascape analysis (Table S9); an overview of the longitudinal study using proteomic techniques revealing the mechanism of SARS-CoV-2 infection in the host (Table S10); clinical parameters of COVID-19 patient at two time points (T1 and T2) (Figure S1); the QC checks of the internal standard (reserpine) for all the samples used in the metabolomic study (Figure S2); box plot of significant metabolites at two time points (severe and nonsevere) (Figure S3); the total number of proteins and peptides detected in the plasma samples (Figure S4); the total number of proteins common and unique in T1 and T2 COVID-19 plasma samples (Figure S5); box plot of significant DEPs in COVID-19 T1 and T2 time points (Figure S6); platelet degranulation pathway (Reactome.Org) (Figure S7); regulation of the complement cascade (Reactome.Org) (Figure S8); platelet activation, signaling, and aggregation (Reactome.Org) (Figure S9); and spiked-in heavy labeled peptide as an internal QC standard for MRM analysis. (A) Representative MRM peaks of the heavy labeled spiked-in peptide (THCLYTHVCDAIK) for a few samples. (B) Bar plot showing the peak areas among all samples. The peak areas of all samples have a CV of 11% and (C) Bar plot showing the consistency in retention times of the spiked-in peptide for all samples (Figure S10) (PDF)

■ AUTHOR INFORMATION

Corresponding Authors

Jayanthi Shastri − *Kasturba Hospital for Infectious Diseases, Mumbai, Maharashtra 400034, India*; Phone: +91-22-2576-7779; Email: jsshastri@gmail.com; Fax: +91-22-2572-3480

Sanjeeva Srivastava − *Department of Biosciences and Bioengineering, Indian Institute of Technology Bombay, Mumbai 400076, India*; orcid.org/0000-0002-0651-4438; Email: sanjeeva@iitb.ac.in

Authors

Kruthi Suvarna − *Department of Biosciences and Bioengineering, Indian Institute of Technology Bombay, Mumbai 400076, India*

Akanksha Salkar − *Department of Biosciences and Bioengineering, Indian Institute of Technology Bombay, Mumbai 400076, India*

Viswanthram Palanivel − *Department of Biosciences and Bioengineering, Indian Institute of Technology Bombay, Mumbai 400076, India*

Renuka Bankar − *Department of Biosciences and Bioengineering, Indian Institute of Technology Bombay, Mumbai 400076, India*

Nirjhar Banerjee − *Department of Biosciences and Bioengineering, Indian Institute of Technology Bombay, Mumbai 400076, India*

Medha Gayathri J Pai − *Department of Biosciences and Bioengineering, Indian Institute of Technology Bombay, Mumbai 400076, India*

Alisha Srivastava − *Department of Biosciences and Bioengineering, Indian Institute of Technology Bombay, Mumbai 400076, India; University of Delhi, New Delhi, Delhi 110021, India*

Avinash Singh − *Department of Biosciences and Bioengineering, Indian Institute of Technology Bombay, Mumbai 400076, India*

Harsh Khatri − *Department of Biosciences and Bioengineering, Indian Institute of Technology Bombay, Mumbai 400076, India*

Sachee Agrawal − *Kasturba Hospital for Infectious Diseases, Mumbai, Maharashtra 400034, India*

Om Shrivastav − *Kasturba Hospital for Infectious Diseases, Mumbai, Maharashtra 400034, India*

Complete contact information is available at: https://pubs.acs.org/10.1021/acs.jproteome.1c00215

Author Contributions

The concept and design of the study were conducted by S.S., J.S., and K.S. Sample collection was done by R.B., V.P., and A.S., and sample preparation was done by K.S., R.B., V.P., and A.S. Mass spectrometry analysis and method optimization were done by K.S. and A.Si. Statistical analysis and data visualization were done by K.S., N.B., A.S., H.K., S.S., and M.G.J. Manuscript writing and review by S.S., K.S., R.B., V.P., A.S., A.Si., M.G.J., N.B., and S.S.

Notes

The authors declare no competing financial interest.

■ ACKNOWLEDGMENTS

The active support from Prof. Ambarish Kunwar from the Department of Biosciences & Bioengineering to fabricate UV transport devices for sample transport and Prof. Anirban Banerjee for the BSL-2 biosafety aspects is gratefully acknowledged. We are also grateful to Dr. Jaishree Garhyan, JNU, New Delhi, for the discussion on biosafety guidelines and Dr. Arup Acharjee, BHU, Varanasi, for the critical discussion on the COVID project. The authors thank Kasturba Hospital for Infectious Diseases for sample collection and sharing sample related information. We also acknowledge efforts of Mr. Abhilash Barpanda for MRM validation experiments. We thank Mr. Gaurish Loya and Mr. Deeptarup Biswas for their valuable inputs and discussion. The study was supported through the Ministry of Science and Technology, Department of Biotechnology, Government of India (BT/PR41020/COT/142/14/2020), and a special COVID seed grant (RD/0520-IRCCHC0-006) from IRCC, IIT Bombay, to S.S. MASSFIITB (Mass Spectrometry Facility, IIT Bombay) from the Department of Biotechnology (BT/PR13114/INF/22/206/2015) is gratefully acknowledged for the MS-based proteomic work.

https://doi.org/10.1021/acs.jproteome.1c00215
J. Proteome Res. XXXX, XXX, XXX−XXX

The authors also acknowledge the Thermo Fisher Scientific engineers and application scientists for their support to our MASSFIITB facility during the extreme lockdown time. The authors acknowledge reactome.org for the pathway figure. K.S. thanks IIT Bombay-IPDF for funding.

REFERENCES

(1) Huang, C.; Wang, Y.; Li, X.; Ren, L.; Zhao, J.; Hu, Y.; Zhang, L.; Fan, G.; Xu, J.; Gu, X.; Cheng, Z.; Yu, T.; Xia, J.; Wei, Y.; Wu, W.; Xie, X.; Yin, W.; Li, H.; Liu, M.; Xiao, Y.; Gao, H.; Guo, L.; Xie, J.; Wang, G.; Jiang, R.; Gao, Z.; Jin, Q.; Wang, J.; Cao, B. Clinical Features of Patients Infected with 2019 Novel Coronavirus in Wuhan, China. *Lancet* **2020**, *395*, 497−506.

(2) Wang, Z.; Deng, H.; Ou, C.; Liang, J.; Wang, Y.; Jiang, M.; Li, S. Clinical Symptoms, Comorbidities and Complications in Severe and Non-Severe Patients with COVID-19: A Systematic Review and Meta-Analysis without Cases Duplication. *Medicine* **2020**, *99*, No. e23327.

(3) Chen, P. L.; Lee, N. Y.; Cia, C. T.; Ko, W. C.; Hsueh, P. R. A Review of Treatment of Coronavirus Disease 2019 (COVID-19): Therapeutic Repurposing and Unmet Clinical Needs. *Front. Pharmacol.* **2020**, *11*, 1−12.

(4) Tarighi, P.; Eftekhari, S.; Chizari, M.; Sabernavaei, M.; Jafari, D.; Mirzabeigi, P. A Review of Potential Suggested Drugs for Coronavirus Disease (COVID-19) Treatment. *Eur. J. Pharmacol.* **2021**, *895*, 173890.

(5) Wiersinga, W. J.; Rhodes, A.; Cheng, A. C.; Peacock, S. J.; Prescott, H. C. Pathophysiology, Transmission, Diagnosis, and Treatment of Coronavirus Disease 2019 (COVID-19): A Review. *JAMA, J. Am. Med. Assoc.* **2020**, *324*, 782−793.

(6) Chang, M. C.; Park, Y. K.; Kim, B. O.; Park, D. Risk Factors for Disease Progression in COVID-19 Patients. *BMC Infect. Dis.* **2020**, *20*, 4−9.

(7) Henry, B. M.; de Oliveira, M. H. S.; Benoit, S.; Plebani, M.; Lippi, G. Hematologic, Biochemical and Immune Biomarker Abnormalities Associated with Severe Illness and Mortality in Coronavirus Disease 2019 (COVID-19): A Meta-Analysis. *Clin. Chem. Lab. Med.* **2020**, *10*, 1021−1028.

(8) Murillo, J.; Villegas, L. M.; Ulloa-Murillo, L. M.; Rodríguez, A. R. Recent Trends on Omics and Bioinformatics Approaches to Study SARS-CoV-2: A Bibliometric Analysis and Mini-Review. *Comput. Biol. Med.* **2021**, *128*, 104162.

(9) Su, Y.; Chen, D.; Yuan, D.; Lausted, C.; Choi, J.; Dai, C. L.; Voillet, V.; Duvvuri, V. R.; Scherler, K.; Troisch, P.; Baloni, P.; Qin, G.; Smith, B.; Kornilov, S. A.; Rostomily, C.; Xu, A.; Li, J.; Dong, S.; Rothchild, A.; Zhou, J.; Murray, K.; Edmark, R.; Hong, S.; Heath, J. E.; Earls, J.; Zhang, R.; Xie, J.; Li, S.; Roper, R.; Jones, L.; Zhou, Y.; Rowen, L.; Liu, R.; Mackay, S.; O'Mahony, D. S.; Dale, C. R.; Wallick, J. A.; Algren, H. A.; Zager, M. A.; Wei, W.; Price, N. D.; Huang, S.; Subramanian, N.; Wang, K.; Magis, A. T.; Hadlock, J. J.; Hood, L.; Aderem, A.; Bluestone, J. A.; Lanier, L. L.; Greenberg, P. D.; Gottardo, R.; Davis, M. M.; Goldman, J. D.; Heath, J. R. Multi-Omics Resolves a Sharp Disease-State Shift between Mild and Moderate COVID-19. *Cell* **2020**, *183*, 1479−1495.

(10) Mahmud, I.; Garrett, T. J. Mass Spectrometry Techniques in Emerging Pathogens Studies: COVID-19 Perspectives. *J. Am. Soc. Mass Spectrom.* **2020**, *31*, 2013−2024.

(11) Suvarna, K.; Biswas, D.; Pai, M. G. J.; Acharjee, A.; Singh, A.; Banerjee, A.; Badaya, A.; Bihani, S.; Loya, G. Proteomics and Machine Learning Approaches Reveal a Set of Prognostic Markers for COVID-19 Severity With Drug Repurposing Potential. *Front. Physiol.* **2021**, *12*, 1−18.

(12) Messner, C. B.; Demichev, V.; Wendisch, D.; Michalick, L.; White, M.; Freiwald, A.; Textoris-Taube, K.; Vernardis, S. I.; Egger, A. S.; Kreidl, M.; Ludwig, D.; Kilian, C.; Agostini, F.; Zelezniak, A.; Thibeault, C.; Pfeiffer, M.; Hippenstiel, S.; Hocke, A.; von Kalle, C.; Campbell, A.; Hayward, C.; Porteous, D. J.; Marioni, R. E.; Langenberg, C.; Lilley, K. S.; Kuebler, W. M.; Mülleder, M.; Drosten, C.; Suttorp, N.; Witzenrath, M.; Kurth, F.; Sander, L. E.; Ralser, M. Ultra-High-Throughput Clinical Proteomics Reveals Classifiers of COVID-19 Infection. *Cell Syst.* **2020**, *11*, 11−24.e4.

(13) Shen, B.; Yi, X.; Sun, Y.; Bi, X.; Du, J.; Zhang, C.; Quan, S.; Zhang, F.; Sun, R.; Qian, L.; Ge, W.; Liu, W.; Liang, S.; Chen, H.; Zhang, Y.; Li, J.; Xu, J.; He, Z.; Chen, B.; Wang, J.; Yan, H.; Zheng, Y.; Wang, D.; Zhu, J.; Kong, Z.; Kang, Z.; Liang, X.; Ding, X.; Ruan, G.; Xiang, N.; Cai, X.; Gao, H.; Li, L.; Li, S.; Xiao, Q.; Lu, T.; Zhu, Y.; Liu, H.; Chen, H.; Guo, T. Proteomic and Metabolomic Characterization of COVID-19 Patient Sera. *Cell* **2020**, *182*, 59−72.

(14) Li, J.; Guo, M.; Li, J.; Guo, M.; Tian, X.; Wang, X.; Yang, X.; Wu, P. Virus-Host Interactome and Proteomic Survey Reveal Potential Virulence Factors Influencing SARS-CoV-2 Pathogenesis. *Med* **2021**, *2*, 99−112.e7.

(15) Demichev, V.; Tober-lau, P.; Nazarenko, T.; Thibeault, C.; Whitwell, H.; Lemke, O.; Röhl, A.; Freiwald, A.; Szyrwiel, L.; Correia-melo, C.; Helbig, E. T.; Stubbemann, P.; Grüning, N.; Blyuss, O.; Vernardis, S.; White, M.; Messner, C. B.; Machleidt, F.; Garcia, C.; Ruwwe-glösenkamp, C.; De Jarcy, L. B.; Stegemann, M. S.; Pfeiffer, M.; Denker, S.; Zickler, D.; Enghard, P.; Zelezniak, A. *A Time-Resolved Proteomic and Diagnostic Map Characterizes COVID-19 Disease Progression and Predicts Outcome*; medRxiv, 2020. https://doi.org/ Overview of longitudinal study using proteomics techniques revealing the mechanism of SARS-CoV-2 infection in the host.

(16) Geyer, P. E.; Arend, F. M.; Doll, S.; Louiset, M.; Virreira Winter, S.; Müller-Reif, J. B.; Torun, F. M.; Weigand, M.; Eichhorn, P.; Bruegel, M.; Strauss, M. T.; Holdt, L. M.; Mann, M.; Teupser, D. *High-Resolution Longitudinal Serum Proteome Trajectories in COVID-19 Reveal Patients-Specific Seroconversion*; medRxiv, 2021, 2021.02.22.21252236.

(17) Bernardes, J. P.; Mishra, N.; Tran, F.; Bahmer, T.; Teichmann, S.; Theis, F.; Wieczorek, D.; Ziebuhr, J. Longitudinal Multi-Omics Analyses Identify Responses of Megakaryocytes, Erythroid Cells, and Plasmablasts as Hallmarks of Severe COVID-19. *Immunity* **2020**, *53*, 1296−1314.e9.

(18) Tyanova, S.; Temu, T.; Cox, J. The MaxQuant Computational Platform for Mass Spectrometry-Based Shotgun Proteomics. *Nat. Protoc.* **2016**, *11*, 2301−2319.

(19) Xia, J.; Sinelnikov, I. V.; Han, B.; Wishart, D. S. MetaboAnalyst 3.0-Making Metabolomics More Meaningful. *Nucleic Acids Res.* **2015**, *43*, W251−W257.

(20) Zhou, Y.; Zhou, B.; Pache, L.; Chang, M.; Khodabakhshi, A. H.; Tanaseichuk, O.; Benner, C.; Chanda, S. K. Metascape Provides a Biologist-Oriented Resource for the Analysis of Systems-Level Datasets. *Nat. Commun.* **2019**, *10*, 1523.

(21) Szklarczyk, D.; Gable, A. L.; Lyon, D.; Junge, A.; Wyder, S.; Huerta-Cepas, J.; Simonovic, M.; Doncheva, N. T.; Morris, J. H.; Bork, P.; Jensen, L. J.; Von Mering, C. STRING V11: Protein-Protein Association Networks with Increased Coverage, Supporting Functional Discovery in Genome-Wide Experimental Datasets. *Nucleic Acids Res.* **2019**, *47*, D607−D613.

(22) Fabregat, A.; Jupe, S.; Matthews, L.; Sidiropoulos, K.; Gillespie, M.; Garapati, P.; Haw, R.; Jassal, B.; Korninger, F.; May, B.; Milacic, M.; Roca, C. D.; Rothfels, K.; Sevilla, C.; Shamovsky, V.; Shorser, S.; Varusai, T.; Viteri, G.; Weiser, J.; Wu, G.; Stein, L.; Hermjakob, H.; D'Eustachio, P. The Reactome Pathway Knowledgebase. *Nucleic Acids Res.* **2018**, *46*, D649−D655.

(23) Perez-Riverol, Y.; Csordas, A.; Bai, J.; Bernal-Llinares, M.; Hewapathirana, S.; Kundu, D. J.; Inuganti, A.; Griss, J.; Mayer, G.; Eisenacher, M.; Pérez, E.; Uszkoreit, J.; Pfeuffer, J.; Sachsenberg, T.; Yilmaz, Ş.; Tiwary, S.; Cox, J.; Audain, E.; Walzer, M.; Jarnuczak, A. F.; Ternent, T.; Brazma, A.; Vizcaíno, J. A. The PRIDE Database and Related Tools and Resources in 2019: Improving Support for Quantification Data. *Nucleic Acids Res.* **2019**, *47*, D442−D450.

(24) Velavan, T. P.; Meyer, C. G. Mild versus Severe COVID-19: Laboratory Markers. *Int. J. Infect. Dis.* **2020**, *95*, 304−307.

(25) Bankar, R.; Suvarna, K.; Ghantasala, S.; Banerjee, A.; Biswas, D.; Choudhury, M.; Palanivel, V.; Salkar, A.; Verma, A.; Singh, A.; Mukherjee, A.; Pai, M.; Roy, J.; Srivastava, A.; Badaya, A.; Agrawal, S.;

https://doi.org/10.1021/acs.jproteome.1c00215
J. Proteome Res. XXXX, XXX, XXX−XXX

Shrivastav, O.; Shastri, J.; Srivastava, S. Proteomic Investigation Reveals Dominant Alterations of Neutrophil Degranulation and MRNA Translation Pathways in Patients with COVID-19. *ISCIENCE* **2021**, *24*, 102135.
(26) Moutchia, J.; Pokharel, P.; Kerri, A.; McGaw, K.; Uchai, S.; Nji, M.; Goodman, M. Clinical Laboratory Parameters Associated with Severe or Critical Novel Coronavirus Disease 2019 (COVID-19): A Systematic Review and Meta-Analysis. *PLoS One* **2020**, *15*, 1−25.
(27) Fraser, D. D.; Slessarev, M.; Martin, C. M.; Daley, M.; Patel, M. A.; Miller, M. R.; Patterson, E. K.; O'Gorman, D. B.; Gill, S. E.; Wishart, D. S.; Mandal, R.; Cepinskas, G. Metabolomics Profiling of Critically Ill Coronavirus Disease 2019 Patients: Identification of Diagnostic and Prognostic Biomarkers. *Crit. Care Explor.* **2020**, *2*, No. e0272.
(28) Cheng, Y.; Luo, R.; Wang, K.; Zhang, M.; Wang, Z.; Dong, L.; Li, J.; Yao, Y.; Ge, S.; Xu, G. Kidney Disease Is Associated with In-Hospital Death of Patients with COVID-19. *Kidney Int.* **2020**, *97*, 829−838.
(29) Andrade Silva, M.; da Silva, A. R. P. A.; do Amaral, M. A.; Fragas, M. G.; Câmara, N. O. S. Metabolic Alterations in SARS-CoV-2 Infection and Its Implication in Kidney Dysfunction. *Front. Physiol.* **2021**, *12*, 624698.
(30) Rosa, A.; Pye, V. E.; Graham, C.; Muir, L.; Seow, J.; Ng, K. W.; Cook, N. J.; Rees-Spear, C.; Parker, E.; dos Santos, M. S.; Rosadas, C.; Susana, A.; Rhys, H.; Nans, A.; Masino, L.; Roustan, C.; Christodoulou, E.; Ulferts, R.; Wrobel, A. G.; Short, C.-E.; Fertleman, M.; Sanders, R. W.; Heaney, J.; Spyer, M.; Kjær, S.; Riddell, A.; Malim, M. H.; Beale, R.; MacRae, J. I.; Taylor, G. P.; Nastouli, E.; van Gils, M. J.; Rosenthal, P. B.; Pizzato, M.; McClure, M. O.; Tedder, R. S.; Kassiotis, G.; McCoy, L. E.; Doores, K. J.; Cherepanov, P. SARS-CoV-2 Can Recruit a Heme Metabolite to Evade Antibody Immunity. *Sci. Adv.* **2021**, *7*, No. eabg7607.
(31) Tang, H. Y.; Wang, C. H.; Ho, H. Y.; Lin, J. F.; Lo, C. J.; Huang, C. Y.; Cheng, M. L. Characteristic of Metabolic Status in Heart Failure and Its Impact in Outcome Perspective. *Metabolites* **2020**, *10*, 437.
(32) Guidetti, G. F.; Torti, M. The Small GTPase Rap1b: A Bidirectional Regulator of Platelet Adhesion Receptors. *J. Signal Transduction* **2012**, *2012*, 1−9.
(33) Stritt, S.; Birkholz, I.; Beck, S.; Sorrentino, S.; Tanuj Sapra, K.; Viaud, J.; Heck, J.; Gaits-Iacovoni, F.; Schulze, H.; Du, X.; Hartwig, J. H.; Braun, A.; Bender, M.; Medalia, O.; Nieswandt, B. Profilin 1−Mediated Cytoskeletal Rearrangements Regulate Integrin Function in Mouse Platelets. *Blood Adv.* **2018**, *2*, 1040−1045.
(34) Cui, G.; Shan, L.; Guo, L.; Chu, I. K.; Li, G.; Quan, Q.; Zhao, Y.; Chong, C. M.; Zhang, Z.; Yu, P.; Hoi, M. P. M.; Sun, Y.; Wang, Y.; Lee, S. M. Y. Novel Anti-Thrombotic Agent for Modulation of Protein Disulfide Isomerase Family Member ERp57 for Prophylactic Therapy. *Sci. Rep.* **2015**, *5*, 10353.
(35) Chamberlain, N.; Korwin-Mihavics, B. R.; Nakada, E. M.; Bruno, S. R.; Heppner, D. E.; Chapman, D. G.; Hoffman, S. M.; van der Vliet, A.; Suratt, B. T.; Dienz, O.; Alcorn, J. F.; Anathy, V. Lung Epithelial Protein Disulfide Isomerase A3 (PDIA3) Plays an Important Role in Influenza Infection, Inflammation, and Airway Mechanics. *Redox Biol.* **2019**, *22*, 101129.
(36) Mayr, M.; Gutmann, C.; Takov, K.; Burnap, S.; Singh, B.; Theofilatos, K.; Reed, E.; Hasman, M.; Nabeebaccus, A.; Fish, M.; McPhail, M.; O'Gallagher, K.; Schmidt, L.; Cassel, C.; Rienks, M.; Yin, X.; Auzinger, G.; Napoli, S.; Mujib, S.; Trovato, F.; Sanderson, B.; Merrick, B.; Niazi, U.; Saqi, M.; Dimitrakopoulou, K.; Braun, S.; Kronstein-Wiedemann, R.; Doores, K.; Edgeworth, J.; Shah, A.; Bornstein, S.; Tonn, T.; Hayday, A.; Shankar-Hari, M. SARS-CoV-2 RNAemia and Proteomic Biomarker Trajectory Inform Prognostication in COVID-19 Patients Admitted to Intensive Care. *ResearchSquare* **2020**, 1−39.
(37) Kenawy, H. I.; Boral, I.; Bevington, A. Complement-Coagulation Cross-Talk: A Potential Mediator of the Physiological Activation of Complement by Low PH. *Front. Immunol.* **2015**, *6*, 215.
(38) Ramlall, V.; Thangaraj, P. M.; Meydan, C.; Foox, J.; Butler, D.; Kim, J.; May, B.; De Freitas, J. K.; Glicksberg, B. S.; Mason, C. E.; Tatonetti, N. P.; Shapira, S. D. Immune Complement and Coagulation Dysfunction in Adverse Outcomes of SARS-CoV-2 Infection. *Nat. Med.* **2020**, *26*, 1609−1615.
(39) Risitano, A. M.; Mastellos, D. C.; Huber-Lang, M.; Yancopoulou, D.; Garlanda, C.; Ciceri, F.; Lambris, J. D. Complement as a Target in COVID-19? *Nat. Rev. Immunol.* **2020**, *20*, 343−344.
(40) D'Alessandro, A.; Thomas, T.; Dzieciatkowska, M.; Hill, R. C.; Francis, R. O.; Hudson, K. E.; Zimring, J. C.; Hod, E. A.; Spitalnik, S. L.; Hansen, K. C. Serum Proteomics in COVID-19 Patients: Altered Coagulation and Complement Status as a Function of IL-6 Level. *J. Proteome Res.* **2020**, *19*, 4417−4427.
(41) Fraga, M.; Moradpour, D.; Artru, F.; Romailler, E.; Tschopp, J.; Schneider, A.; Chtioui, H.; Neerman-Arbez, M.; Casini, A.; Alberio, L.; Sempoux, C. Hepatocellular Type II Fibrinogen Inclusions in a Patient with Severe COVID-19 and Hepatitis. *J. Hepatol.* **2020**, *73*, 967−970.
(42) Ruberto, F.; Chistolini, A.; Curreli, M.; Frati, G.; Marullo, A. G. M.; Biondi-Zoccai, G.; Mancone, M.; Sciarretta, S.; Miraldi, F.; Alessandri, F.; Ceccarelli, G.; Barone, F.; Santoro, C.; Alvaro, D.; Pugliese, F.; Bruno, K.; Cappannoli, A.; Cardinale, V.; Celli, P.; Consolo, S.; Croce, C.; Crocitti, B.; D'Ettorre, G.; Maldarelli, F.; Martelli, S.; Mastroianni, C.; Messina, T.; Pattelli, E.; Pecorari, F.; Perrella, S.; Piazzolla, M.; Portieri, M.; Pulcinelli, F. M.; Ratini, F.; Ricci, C.; Santopietro, P.; Tellan, G.; Titi, L.; Tordiglione, P.; Tosi, A.; Trigilia, F. Von Willebrand Factor with Increased Binding Capacity Is Associated with Reduced Platelet Aggregation but Enhanced Agglutination in COVID-19 Patients: Another COVID-19 Paradox? *J. Thromb. Thrombolysis* **2021**, *Jan*, 105−110.
(43) Stegelmeier, A. A.; van Vloten, J. P.; Mould, R. C.; Klafuric, E. M.; Minott, J. A.; Wootton, S. K.; Bridle, B. W.; Karimi, K. Myeloid Cells during Viral Infections and Inflammation. *Viruses* **2019**, *11*, 168.
(44) Schulte-Schrepping, J.; Reusch, N.; Paclik, D.; Baßler, K.; Schlickeiser, S.; Zhang, B.; Makarewicz, O.; Marz, M.; McHardy, A.; Stegle, O.; Stoye, J.; Theis, F.; Vehreschild, J.; Vogel, J.; von Kleist, M.; Walker, A.; Walter, J.; Wieczorek, D.; Ziebuhr, J. Severe COVID-19 Is Marked by a Dysregulated Myeloid Cell Compartment. *Cell* **2020**, *182*, 1419−1440.e23.
(45) Burrack, K. S.; Morrison, T. E. The Role of Myeloid Cell Activation and Arginine Metabolism in the Pathogenesis of Virus-Induced Diseases. *Front. Immunol.* **2014**, *5*, 248.
(46) Rodriguez, P. C.; Ochoa, A. C.; Al-Khami, A. A. Arginine Metabolism in Myeloid Cells Shapes Innate and Adaptive Immunity. *Front. Immunol.* **2017**, *8*, 93.
(47) Thomas, T.; Stefanoni, D.; Reisz, J. A.; Nemkov, T.; Bertolone, L.; Francis, R. O.; Hudson, K. E.; Zimring, J. C.; Hansen, K. C.; Hod, E. A.; Spitalnik, S. L.; D'Alessandro, A. COVID-19 Infection Alters Kynurenine and Fatty Acid Metabolism, Correlating with IL-6 Levels and Renal Status. *JCI Insight* **2020**, *5*, No. e140327.
(48) Kimhofer, T.; Lodge, S.; Whiley, L.; Gray, N.; Loo, R. L.; Lawler, N. G.; Nitschke, P.; Bong, S.-H.; Morrison, D. L.; Begum, S.; Richards, T.; Yeap, B. B.; Smith, C.; Smith, K. G. C.; Holmes, E.; Nicholson, J. K. Integrative Modeling of Quantitative Plasma Lipoprotein, Metabolic, and Amino Acid Data Reveals a Multiorgan Pathological Signature of SARS-CoV-2 Infection. *J. Proteome Res.* **2020**, *19*, 4442−4454.
(49) Blasco, H.; Bessy, C.; Plantier, L.; Lefevre, A.; Piver, E.; Bernard, L.; Marlet, J.; Stefic, K.; Benz-de Bretagne, I.; Cannet, P.; Lumbu, H.; Morel, T.; Boulard, P.; Andres, C. R.; Vourc'h, P.; Hérault, O.; Guillon, A.; Emond, P. The Specific Metabolome Profiling of Patients Infected by SARS-COV-2 Supports the Key Role of Tryptophan-Nicotinamide Pathway and Cytosine Metabolism. *Sci. Rep.* **2020**, *10*, 16824.
(50) Barberis, E.; Timo, S.; Amede, E.; Vanella, V. V.; Puricelli, C.; Cappellano, G.; Raineri, D.; Cittone, M. G.; Rizzi, E.; Pedrinelli, A. R.; Vassia, V.; Casciaro, F. G.; Priora, S.; Nerici, I.; Galbiati, A.; Hayden, E.; Falasca, M.; Vaschetto, R.; Sainaghi, P. P.; Dianzani, U.; Rolla, R.; Chiocchetti, A.; Baldanzi, G.; Marengo, E.; Manfredi, M. Large-Scale

https://doi.org/10.1021/acs.jproteome.1c00215
J. Proteome Res. XXXX, XXX, XXX−XXX

Plasma Analysis Revealed New Mechanisms and Molecules Associated with the Host Response to Sars-Cov-2. *Int. J. Mol. Sci.* **2020**, *21*, 8623.

(51) Ansone, L.; Ustinova, M.; Terentjeva, A.; Perkons, I.; Birzniece, L.; Rovite, V.; Rozentale, B.; Viksna, L.; Kolesova, O.; Klavins, K.; Klovins, J. Tryptophan and Arginine Metabolism Is Significantly Altered at the Time of Admission in Hospital for Severe COVID-19 Patients: Findings from Longitudinal Targeted Metabolomics Analysis. *medRxiv* **2021**, *April* (). DOI: 10.1101/2021.03.31.21254699.

(52) Xiao, N.; Nie, M.; Pang, H.; Wang, B.; Hu, J.; Meng, X.; Li, K.; Ran, X.; Long, Q.; Deng, H.; Chen, N.; Li, S.; Tang, N.; Huang, A.; Hu, Z. Integrated Cytokine and Metabolite Analysis Reveals Immunometabolic Reprogramming in COVID-19 Patients with Therapeutic Implications. *Nat. Commun.* **2021**, *12*, 1618.

(53) Hughes, D. A.; Norton, R. Vitamin D and Respiratory Health. *Clin. Exp. Immunol.* **2009**, *158*, 20−25.

(54) Speeckaert, M. M.; Delanghe, J. R. A Key Role for Vitamin D Binding Protein in COVID - 19? *Eur. J. Nutr.* **2021**, *60*, 2259−2260.

https://doi.org/10.1021/acs.jproteome.1c00215
J. Proteome Res. XXXX, XXX, XXX−XXX